

# Location of Subcortical Microbleeds and Recovery of Consciousness After Severe Traumatic Brain Injury

Marta Bianciardi, PhD, Saef Izzy, MD, Bruce R. Rosen, MD, PhD, Lawrence L. Wald, PhD, and Brian L. Edlow, MD

*Neurology*® 2021;97:e113-e123. doi:10.1212/WNL.00000000000012192

## Correspondence

Dr. Bianciardi  
martab@mgh.harvard.edu

## Abstract

### Background

In patients with severe traumatic brain injury (TBI), coma is associated with impaired subcortical arousal mechanisms. However, it is unknown which nuclei involved in arousal (arousal nuclei) are implicated in coma pathogenesis and are compatible with coma recovery.

### Methods

We mapped an atlas of arousal nuclei in the brainstem, thalamus, hypothalamus, and basal forebrain onto 3 tesla susceptibility-weighted images (SWI) in 12 patients with acute severe TBI who presented in coma and recovered consciousness within 6 months. We assessed the spatial distribution and volume of SWI microbleeds and evaluated the association of microbleed volume with the duration of unresponsiveness and functional recovery at 6 months.

### Results

There was no single arousal nucleus affected by microbleeds in all patients. Rather, multiple combinations of microbleeds in brainstem, thalamic, and hypothalamic arousal nuclei were associated with coma and were compatible with recovery of consciousness. Microbleeds were frequently detected in the midbrain (100%), thalamus (83%), and pons (75%). Within the brainstem, the microbleed incidence was largest within the mesopontine tegmentum (e.g., pedunculotegmental nucleus, mesencephalic reticular formation) and ventral midbrain (e.g., substantia nigra, ventral tegmental area). Brainstem arousal nuclei were partially affected by microbleeds, with microbleed volume not exceeding 35% of brainstem nucleus volume on average. Compared to microbleed volume within nonarousal brainstem regions, the microbleed volume within arousal brainstem nuclei accounted for a larger proportion of variance in the duration of unresponsiveness and 6-month Glasgow Outcome Scale–Extended scores.

### Conclusion

These results suggest resilience of arousal mechanisms in the human brain after severe TBI.

## RELATED ARTICLE

### Editorial

Good Recovery Is Possible in Young Patients With Posttraumatic Coma and Brainstem Microbleeds

Page 53

## MORE ONLINE

### CME Course

[NPub.org/cmelist](https://www.npub.org/cmelist)

From the Department of Radiology, Athinoula A. Martinos Center for Biomedical Imaging (M.B., B.R.R., L.L.W., B.L.E.), and Center for Neurotechnology and Neurorecovery, Department of Neurology (B.L.E.), Massachusetts General Hospital and Harvard Medical School; Division of Sleep Medicine (M.B.), Harvard University; and Department of Neurology (S.I.), Brigham and Women's Hospital and Harvard Medical School, Boston, MA.

Go to [Neurology.org/N](https://www.neurology.org/N) for full disclosures. Funding information and disclosures deemed relevant by the authors, if any, are provided at the end of the article.

## Glossary

**CLi** = caudal linear raphe; **CnF** = cuneiform nucleus; **DR** = dorsal raphe; **GCS** = Glasgow Coma Scale; **GOSE** = Glasgow Outcome Scale–Extended; **ICU** = intensive care unit; **isRt** = isthmus reticular formation; **LC** = locus coeruleus; **LDTg** = laterodorsal tegmental nucleus; **MEMPRAGE** = multiecho magnetization-prepared rapid gradient echo; **MNI** = Montreal Neurological Institute; **MnR** = median raphe; **mRt-p1Rt** = mesencephalic reticular formation and p1 reticular formation; **PAG** = periaqueductal gray; **PMnR** = paramedian raphe nucleus; **PTg** = pedunculotegmental nucleus; **SN** = substantia nigra; **SWI** = susceptibility-weighted imaging; **T1W** = T1-weighted; **TBI** = traumatic brain injury; **VTA-PBP** = ventral tegmental area with parabrachial pigmented nucleus.

In patients with severe traumatic brain injury (TBI), coma is believed to be caused by disruption of an ascending arousal network<sup>1-4</sup> that links arousal nuclei in the brainstem, thalamus, hypothalamus, and basal forebrain to the cerebral cortex.<sup>5-7</sup> However, due to difficulty in localizing these nuclei with conventional MRI, the specific nuclei whose injury is implicated in the pathogenesis of traumatic coma have not been identified. Moreover, it is unknown which arousal nuclei can be lesioned and still compatible with recovery of consciousness. These gaps in knowledge have profound clinical implications for patients with severe TBI. Without knowing whether a patient can recover consciousness, many families withdraw life-sustaining treatment, a decision that accounts for up to 70% of deaths for patients with severe TBI in the intensive care unit (ICU).<sup>8,9</sup>

This study aimed to identify the combinations of arousal nuclei affected by microbleeds that are associated with coma and are compatible with recovery of consciousness in patients with acute severe TBI. We enrolled patients presenting in traumatic coma and performed susceptibility-weighted imaging (SWI) to identify microbleeds, the radiologic hallmark of hemorrhagic traumatic axonal injury.<sup>2,10</sup> We then integrated SWI microbleed maps with brainstem, thalamic, hypothalamic, and basal forebrain atlases. Using this atlas-based approach, we mapped the neuroanatomic location of subcortical microbleeds that are associated with traumatic coma and compatible with recovery of consciousness. As a control, we performed similar SWI microbleed analyses on a cohort of patients with moderate TBI.

## Methods

### Standard Protocol Approvals, Registrations, and Patient Consents

For the 16 patients with severe TBI who were enrolled in this study, surrogate decision-makers provided written informed consent in accordance with an institutional review board–approved protocol. The cohort was enrolled during the pilot phase of a multimodal study examining predictors of recovery from severe TBI (ClinicalTrials.gov; NCT03504709); thus, the cohort size for this descriptive study was not determined using a power calculation. The 12-patient moderate TBI cohort was identified retrospectively using a separate institutional review board–approved protocol, for which written consent was waived.

### Recruitment and Study Procedures for Patients With Severe TBI

We prospectively and consecutively screened all patients with TBI admitted to the ICU at an academic hospital over 3 years. We enrolled 16 patients with severe TBI (12 M/4 F, mean  $\pm$  SE age  $29 \pm 2$  years) who met criteria for coma: initial Glasgow Coma Scale (GCS) total score  $\leq 6$ , with no eye-opening or verbal response for at least 24 hours on examinations unconfounded by sedation or paralysis.

All patients with severe TBI underwent SWI MRI as soon as they were stable to travel to the MRI scanner, as determined by treating clinicians. We defined the duration of unresponsiveness by the time from TBI to command-following. We acknowledge that command-following is not the only behavioral sign of responsiveness in this patient population, as eye-gaze tracking and localization to noxious stimuli also indicate emergence from coma to the minimally conscious state.<sup>11</sup> Nevertheless, we used command-following as the primary outcome measure for early emergence from coma because this is a commonly used measure of responsiveness in studies of patients with acute severe TBI.<sup>12-14</sup> At 6-month follow-up, we defined full recovery of consciousness as emergence from the posttraumatic confusional state, based on Confusional Assessment Protocol criteria. We also assessed functional outcome using the Glasgow Outcome Scale–Extended (GOSE).

Of the 16 patients, 2 were excluded because they died in the ICU after surrogate decision-makers withdrew life-sustaining therapy, and 2 others were excluded because of motion artifacts identified by an investigator blinded to the clinical data (M.B.). Twelve fully recovered consciousness by 6 months (9 M/3 F, age  $26 \pm 2$  years) and were included in this study (table).

### SWI Data Acquisition

Patients underwent 3D SWI on a 3 tesla Skyra scanner (Siemens-Healthineers; 32-channel head-coil) with spatial resolution =  $0.86 \times 0.86 \times 1.8$  mm<sup>3</sup>, repetition time = 30 ms, echo time = 20 ms, flip angle = 15°, bandwidth = 120 Hz/pixel, acquisition time = 4 minutes 33 seconds. For coregistration, a 3D T1-weighted (T1W) multiecho magnetization-prepared rapid gradient echo (MEMPRAGE) was acquired with 1 mm isotropic spatial resolution, repetition time = 2.53 seconds, echo times = 1.69/3.55/5.41/7.27 ms, inversion time = 1.2 seconds, flip angle = 7°, and GRAPPA factor = 3.

**Table** Patient Demographics and Outcome Measures

Patient number	Age at time of injury, y	Sex	Mechanism of injury	Duration of unresponsiveness, d	GOSE 6 months post TBI (1 = death; 8 = upper good recovery)
1	27	M	Motor vehicle accident	1	3
2	21	M	Pedestrian hit by car	6	7
3	19	F	Motor vehicle accident	14	7
4	28	F	Motor vehicle accident	9	3
5	45	M	Motor vehicle accident	6	5
6	33	M	Fall	7	3
7	24	M	Assault	7	5
8	22	F	Pedestrian hit by car	9	7
9	18	M	Fall	2	7
10	29	M	Pedestrian hit by car	8	5
11	19	M	Fall	2	7
12	32	M	Pedestrian hit by car	8	4

Abbreviations: GOSE = Glasgow Outcome Scale–Extended; TBI = traumatic brain injury.

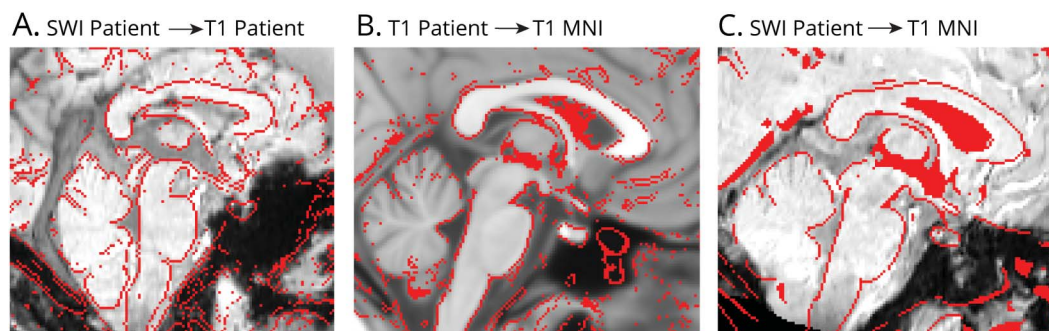
The variable timing of SWI data acquisition (i.e., depending on clinician judgment about the safety of traveling to the MRI scanner) created the possibility that patients might emerge from coma prior to the SWI MRI. However, the number and size of traumatic microbleeds detected by SWI is not expected to vary with time. Rather, evidence suggests that the magnetic susceptibility effect of blood measured by the MRI scanner is consistent over a time course of hours to days,<sup>15</sup> as long as the

data are acquired using the same MRI scanner field strength and SWI sequence.<sup>16</sup>

### SWI Data Coregistration to Stereotactic Space

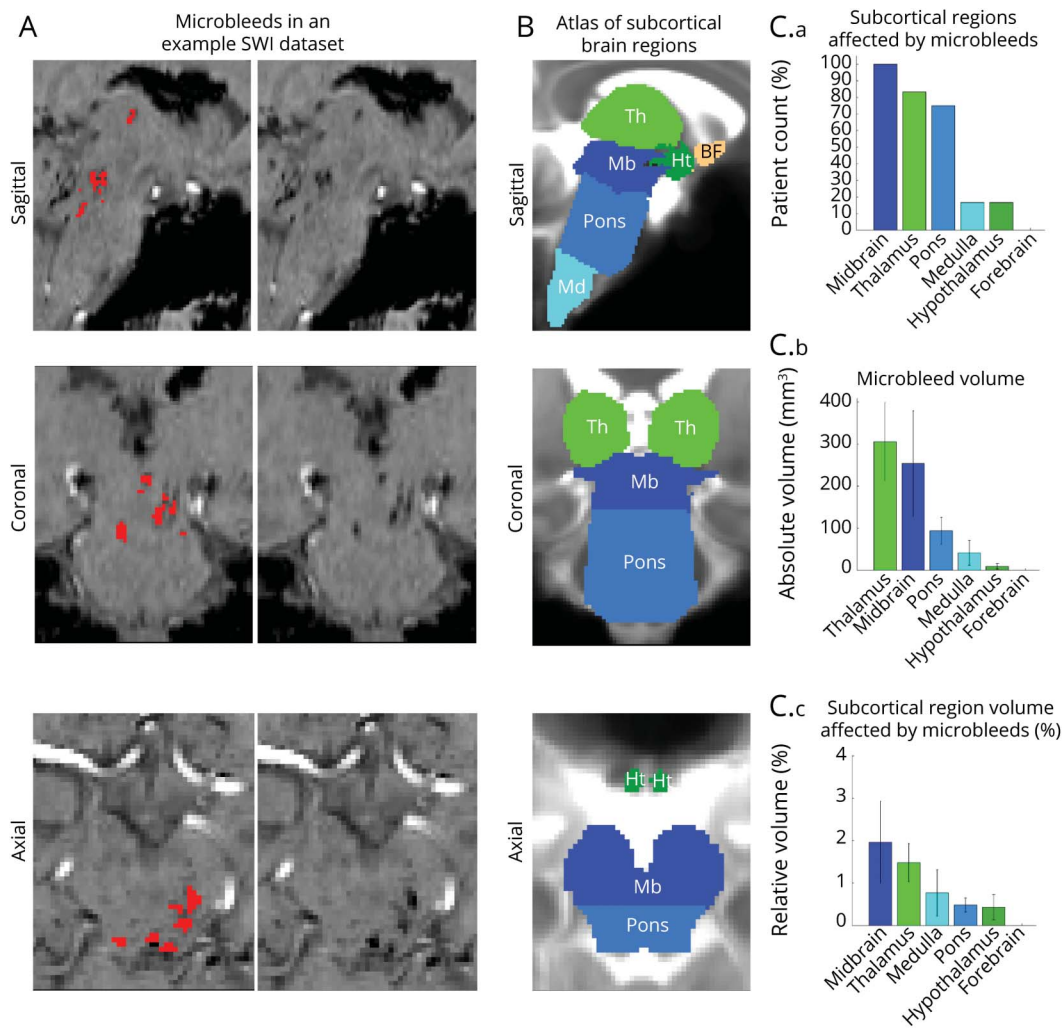
After bias-field correction, each patient's SWI dataset was precisely coregistered to the nonlinear 6th-generation T1W-Montreal Neurological Institute (MNI) 152 template by concatenating and applying the following transformations

**Figure 1** Coregistration of Susceptibility-Weighted Imaging (SWI) Data to Stereotactic Space



We concatenated 2 steps (A, B) to perform the coregistration to stereotactic Montreal Neurologic Institute (MNI) space (C). Coregistration results are shown for an example dataset. (A) Overlay (red lines) of the single-patient SWI dataset coregistered to the single-patient T1-weighted multiecho magnetization-prepared rapid gradient echo (T1 patient). (B) Overlay (red lines) of the T1 patient image (coregistered to the T1-weighted MNI152 standard template; T1 MNI) on the T1 MNI template. (C) Overlay (red lines) of the single-patient SWI dataset (coregistered to the T1 MNI template by combining the transformations used in A and B) on the T1 MNI template. These images demonstrate that precise coregistration was achieved in the subcortical regions that were analyzed in this study. Similar coregistration performance was achieved for the other 11 patients.

**Figure 2** Evaluation of Microbleeds in Subcortical Arousal Regions



(A) An example susceptibility-weighted imaging (SWI) dataset in stereotactic Montreal Neurologic Institute (MNI) space is shown along with manually delineated microbleeds (red), identified as SWI hypointensities within a microbleed search-mask. (B) Overlaid on a T2-weighted image in stereotactic space, we show the traumatic microbleed search-mask including regions involved in arousal, such as the brainstem (midbrain [Mb], dark blue; pons, light blue; and medulla [Md], cyan), thalamus (Th) (light green), hypothalamus (Ht) (dark green), and basal forebrain (BF) (copper). (C.a) Count of patients with deep arousal regions affected by microbleeds (range 0%–100%, corresponding to 0–12 patients). (C.b) Volume of microbleeds within each deep arousal region. (C.c) Volume of microbleeds (within each deep arousal region) relative to the volume of each region. Note the higher incidence and volume of microbleeds in the midbrain, thalamus, and pons compared to the medulla and hypothalamus (no occurrence in the BF), and the relatively small fraction of deep region volume affected by microbleeds.

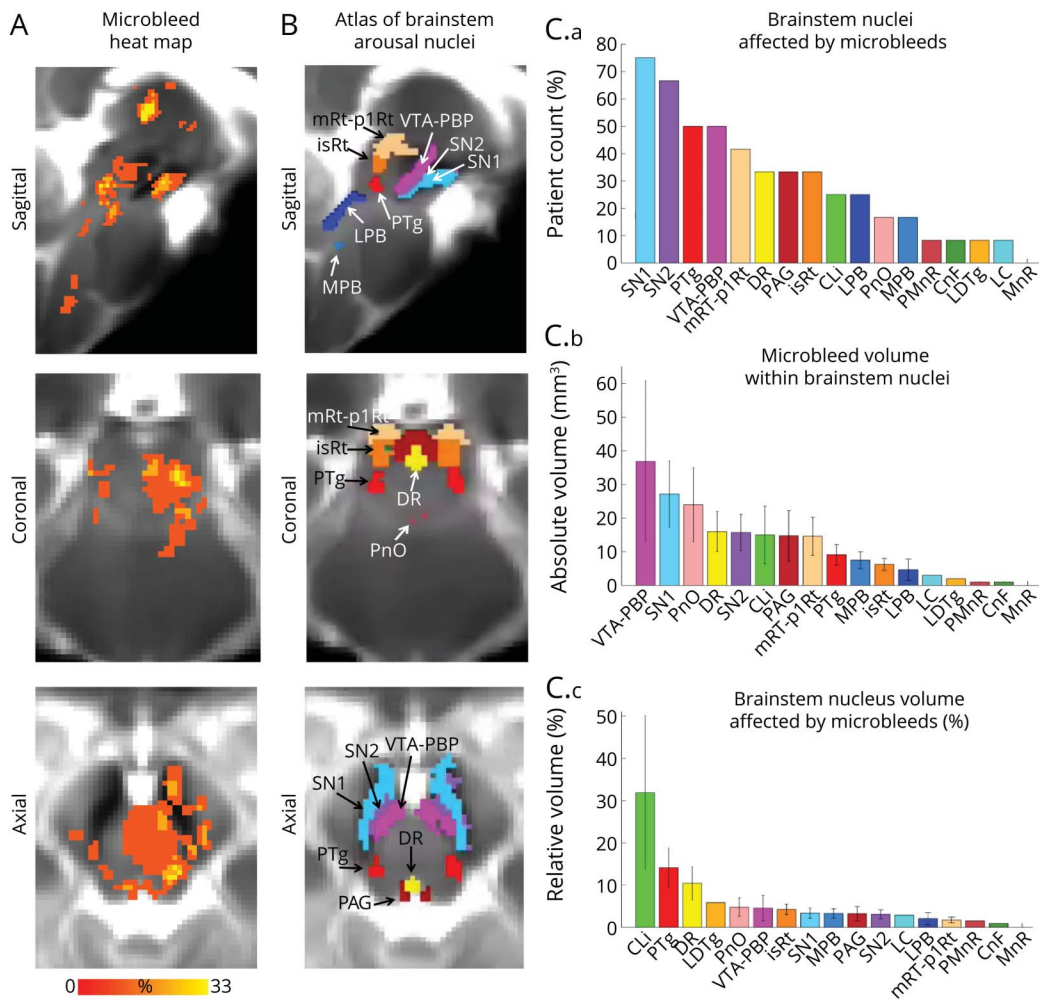
(Advanced Normalization Tool): the 12 degrees of freedom affine-transformation (metric: mutual information) computed to coregister the SWI to the T1W-MEMPRAGE; and the high-dimensional nonlinear transformation (metric: cross correlation) computed to coregister the T1W-MEMPRAGE to the T1W-MNI152. In figure 1, A–C, we show the coregistration procedure and its performance in an example dataset.

### SWI Data Analysis

After coregistration, we defined a “traumatic microbleed search mask” (figure 2B), comprising the thalamus,<sup>17</sup> hypothalamus,<sup>18</sup> basal forebrain (including nucleus accumbens<sup>17</sup> and other manually delineated subregions), and the brainstem (medulla,<sup>19,20</sup> pons,<sup>19</sup> and midbrain<sup>20</sup>). The mask of the pons

(figure 2B) was generated by applying automated segmentation procedures<sup>19</sup> to the 1 mm resolution T1W MNI152 template. To generate the mask of the medulla and midbrain, we first generated a brainstem mask using the FreeSurfer parcellation<sup>20</sup> of the 1 mm resolution T1W MNI152 template. The mask of the medulla (figure 2B) was defined using the inferior boundary of the pontine mask as the superior boundary of the medulla. Finally, the mask of the midbrain was initialized as the superior part of the brainstem mask, using the superior boundary of the pontine mask as the inferior boundary of the midbrain. The mask of the midbrain was then manually edited by M.B. (figure 2B) to include parts of the rostral midbrain that are absent in the FreeSurfer parcellation. Diencephalic regions such as the subthalamic nucleus<sup>21</sup> were excluded.

**Figure 3** Evaluation of Microbleeds in Brainstem Arousal Nuclei



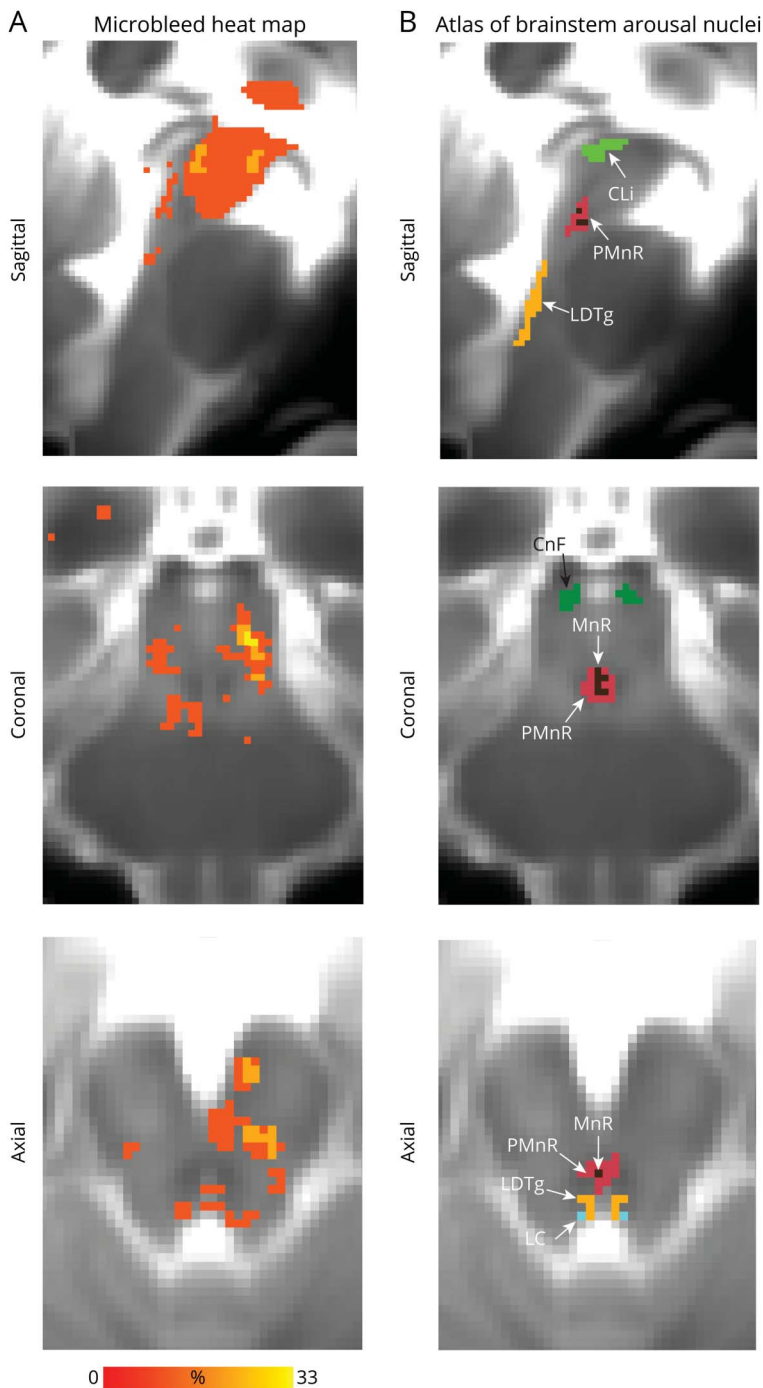
(A) Spatial overlap of microbleeds across patients at the voxel level in the form of a heat map. Microbleeds were mainly present in the thalamus and in the upper brainstem (midbrain and pons), yet their overlap at the voxel level was less than 33%. (B) Atlas of 17 arousal brainstem nuclei used to evaluate microbleed overlap at the nucleus level. (C.a) Count of patients with brainstem arousal nuclei affected by microbleeds (descending order, range 0%–100%, corresponding to 0–12 patients). (C.b) Volume of microbleeds within each brainstem nucleus (descending order). (C.c) Volume of microbleeds within each brainstem nucleus relative to the volume of each brainstem nucleus (descending order). Note that some brainstem nuclei (substantia nigra subregion 1 [compatible with pars reticulata] [SN1], substantia nigra subregion 2 [compatible with pars compacta] [SN2], pedunculotegmental nucleus [also known as pedunculopontine nucleus] [PTg], ventral tegmental area with parabrachial pigmented nucleus [VTA-PBP], mesencephalic reticular formation and p1 reticular formation [mRt-p1Rt], dorsal raphe [DR], periaqueductal gray [PAG], isthmic reticular formation [isRt]) displayed an incidence of microbleeds higher than 30%, yet only a relatively small fraction of the brainstem nuclei volume was affected by microbleeds. CLI = caudal linear raphe; CnF = cuneiform nucleus; LC = locus coeruleus; LDTg = laterodorsal tegmental nucleus; LPB = lateral parabrachial nucleus; MnR = median raphe; MPB = medial parabrachial nucleus; PMnR = paramedian raphe nucleus; PnO = pontine reticular nucleus, oral part.

Within the microbleed search mask, a trained microbleed rater (S.I.) manually delineated signal hypointensities (i.e., presumptive traumatic microbleeds) on the patients' SWI datasets in MNI152 space using established methods.<sup>22,23</sup> We assessed the spatial distribution and overlap of traumatic microbleeds at the voxel level by computing the sum of microbleeds within each voxel across patients. Further, we evaluated the spatial distribution and overlap of microbleeds across patients at the nucleus/region level by counting the number of patients with microbleeds in each nucleus/region, the volume of microbleeds within each nucleus/region, and the percentage nucleus/region volume affected by microbleeds. For this analysis, we considered 6

regions (thalamus, hypothalamus, basal forebrain, midbrain, pons, medulla; figure 2B) and 17 brainstem nuclei postulated to modulate arousal based on animal studies (see next section). We defined a control region (primarily involved in functions other than arousal) as the whole brainstem excluding the 17 arousal nuclei.

We also performed a post hoc analysis of the volume of microbleeds in the 2 patients who died due to withdrawal of life-sustaining therapy. Our goal was to assess for differences in microbleed characteristics between the 2 patients with severe TBI who died in the ICU and the 12 patients with severe TBI who survived.

**Figure 4** Evaluation of Microbleeds in Brainstem Arousal Nuclei



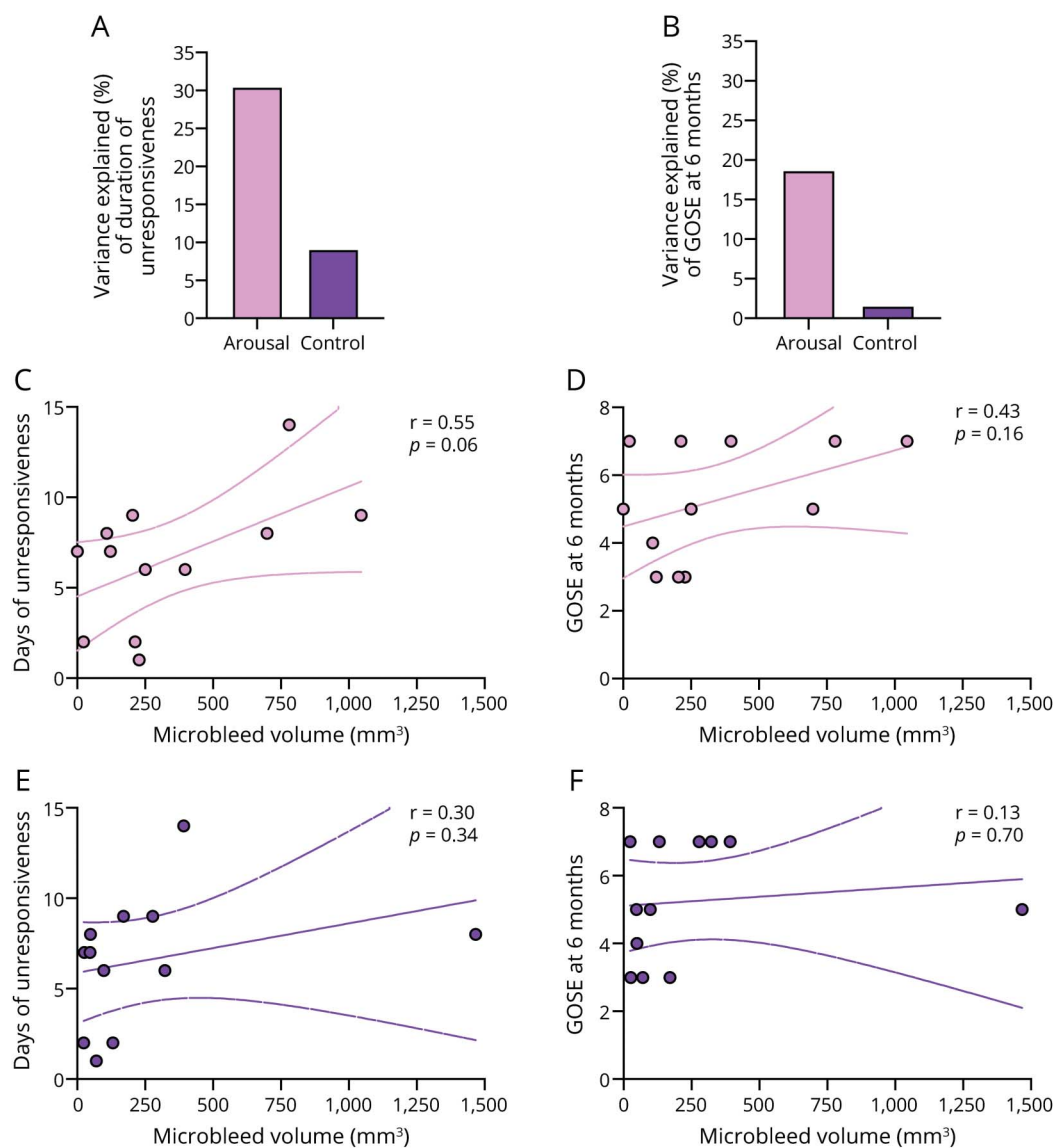
Additional views of 6 brainstem nuclei (caudal linear raphe [CLi], paramedian raphe nucleus [PMnR], cuneiform nucleus [CnF], laterodorsal tegmental nucleus [LDTg], locus coeruleus [LC], median raphe [MnR]), which are not visible in figure 3. (A) Spatial overlap of microbleeds across patients at the voxel level in the form of a heat map. (B) Atlas of arousal brainstem nuclei used to evaluate the microbleed overlap at the nucleus level.

### Selection and Definition of Brainstem Nuclei Labels

The 17 brainstem arousal nuclei analyzed in this study were selected based on several lines of evidence: (1) lesion/stimulation studies in animals; (2) anatomical mapping studies in animals and humans showing direct connections to the cortex or indirect connections through the thalamus, hypothalamus, and basal forebrain; (3) coma studies in humans and animals. These arousal nuclei include meso-pontine

reticular formation nuclei<sup>5,24</sup> (such as the mesencephalic reticular formation, cuneiform nucleus, isthmus reticular formation, and pontine reticular formation), cholinergic nuclei<sup>5,6,25</sup> (such as the pedunculotegmental and laterodorsal tegmental nucleus), serotonergic raphe nuclei<sup>5,6,25</sup> (such as dorsal, median, paramedian, and caudal-linear raphe), and noradrenergic locus coeruleus.<sup>5,6,25</sup> Moreover, prior studies indicate that autonomic and visceral nuclei (such as the periaqueductal gray<sup>5,25</sup> and the lateral/medial parabrachial

**Figure 5** Correlation of Microbleed Volume With Coma Outcome Measures



(A, B) Variance of clinical outcome measures. (A) Duration of unresponsiveness, defined by time until command-following. (B) Glasgow Outcome Scale-Extended (GOSE) at 6 months after the traumatic brain injury (TBI) explained by the microbleed volume within all nuclei/regions involved in arousal (i.e., thalamus, hypothalamus, basal forebrain, and 17 brainstem nuclei) was higher than the variance explained by the microbleed volume within the control region (i.e., the brainstem excluding the 17 brainstem nuclei involved in arousal). (C, D) Total microbleed volume evaluated in all nuclei/regions involved in arousal across participants versus (C) duration of unresponsiveness (Pearson correlation coefficient  $r = 0.55$ ,  $p = 0.06$ ) and (D) GOSE at 6 months after the TBI ( $r = 0.43$ ,  $p = 0.16$ ). (E, F) Total microbleed volume evaluated in the control region across participants versus (E) duration of unresponsiveness (Pearson correlation coefficient  $r = 0.30$ ,  $p = 0.34$ ) and (F) GOSE at 6 months after the TBI ( $r = 0.13$ ,  $p = 0.70$ ).

nuclei<sup>6,25-27</sup>) are involved in modulating arousal. Finally, mesolimbic dopaminergic nuclei (such as the ventral tegmental area<sup>5,28,29</sup> and substantia nigra<sup>30-33</sup> complex) appear to modulate arousal, based on their anatomical connections as well as stimulation studies in animals.

The complete list of 17 brainstem arousal nuclei that we analyzed is as follows: mesencephalic reticular formation and p1 reticular formation (mRt-p1Rt), cuneiform nucleus (CnF), isthmus reticular formation (isRt), pontine reticular formation oral (and the smaller caudal) part (PnO), pedunculotegmental nucleus (PTg), laterodorsal tegmental nucleus (LDTg), dorsal raphe

(DR), median raphe (MnR), paramedian-raphé (PMnR), caudal-linear raphe (CLi), locus coeruleus (LC), periaqueductal gray (PAG), lateral/medial parabrachial nuclei (LPB, MPB), ventral tegmental area with parabrachial pigmented nucleus (VTA-PBP), and 2 subnuclei of the substantia nigra (SN1/2, compatible respectively with pars reticulata/compacta). Specifically, we used probabilistic atlas labels of these nuclei developed by our group in living humans using ultra-high-field multi-contrast MRI<sup>21,34,35</sup> thresholded at 35% and binarized to yield masks defining the location of these nuclei in SWI coregistered to stereotactic (MNI) space. Of note, left- and right-sided nuclei/regions were combined for the analyses.

## Moderate TBI Patient Cohort

As a control to the severe TBI patient cohort, we investigated SWI microbleeds in patients with moderate TBI ( $n = 12$ , 8 M/4 F, mean  $\pm$  SE age  $55 \pm 5$  years). Patients in the moderate TBI cohort (initial GCS scores 9–12) were scanned on the same 3T MRI scanner, with the same SWI sequence and during the same 3-year period as the severe TBI cohort.

## Correlations Between Microbleeds and Clinical Outcomes

We performed a Pearson correlation analysis to test for associations between clinical outcome measures (i.e., duration of unresponsiveness and 6-month GOSE score) and the volume of microbleeds within all nuclei/regions involved in arousal (i.e., thalamus, hypothalamus, basal forebrain, and 17 brainstem nuclei). We also tested for correlations between the control (i.e., nonarousal) region and the clinical outcome measures.

## Data Availability

Anonymized SWI data will be shared by request from any qualified investigator.

## Results

### Microbleed Neuroanatomic Characteristics in Acute Severe TBI

A representative SWI microbleed delineation is shown in figure 2A. At the group level, the midbrain was affected by microbleeds in all patients, the thalamus in 83%, the pons in 75%, the hypothalamus and the medulla in 17% (figure 2). No patient had basal forebrain microbleeds. The total volume of microbleeds was highest in the thalamus and midbrain, followed by the pons, medulla, and hypothalamus (figure 2C).

Microbleed overlap across patients at the voxel level was moderate ( $\leq 33\%$ ; figure 3A). However, we observed a high incidence of microbleed overlap at the nucleus level (figure 3C), especially for SN1, SN2, PTg, VTA-PBP, mRt-p1Rt, DR, PAG, and isRt. No single brainstem arousal nucleus was lesioned by microbleeds in the whole cohort (i.e., maximum peak incidence was 75%). Moreover, brainstem arousal nuclei were only partially affected (figure 3C), with microbleed volume not exceeding 35% of brainstem nucleus volume on average. In figure 4, A and B, we show additional views of the microbleed overlap for CLi, PMnR, CnF, LC, MnR, and LDTg nuclei, not visible in figure 3, A and B.

### Clinical Correlations With Microbleeds in Acute Severe TBI

Total microbleed volume within all arousal nuclei/regions explained more variance in clinical outcome measures than did the volume of microbleeds in the control region (figure 5, A and B). The former also displayed a trend toward correlation with duration of unresponsiveness ( $R = 0.55$ ,  $p = 0.06$ ) but not with GOSE scores at 6 months (figure 5, C and D).

## Microbleed Volume in Subcortical Regions in Patients With Severe TBI Who Died After Withdrawal of Life-Sustaining Therapy

The 2 patients who died after withdrawal of life-sustaining therapy had a microbleed volume in the thalamus, hypothalamus, basal forebrain, and brainstem of 126 and 234  $\text{mm}^3$ , respectively. These volumes are within the range of microbleed volumes in the thalamus, hypothalamus, basal forebrain, and brainstem in the 12 patients who recovered consciousness (range 47–2,140  $\text{mm}^3$ ). Of note, the decision to withdraw life-sustaining therapy in these patients was not based solely on the presence of subcortical microbleeds. Rather, these decisions were also influenced by the presence of a large (>100 mL) right frontal contusion in one patient and the presence of preexisting psychiatric illness in the other patient.

## Comparison of Microbleed Incidence and Anatomic Location Between Patients With Moderate and Severe TBI

In the moderate TBI cohort, the incidence and volume of microbleeds in arousal regions (figure 6) was lower for each region than in the severe TBI cohort. For example, only 30% of patients with moderate TBI had microbleeds in the midbrain (figure 6A), compared to 100% of patients with severe TBI (figure 2C, top panel). Moreover, the absolute average volume of microbleeds in the midbrain in the moderate TBI cohort (figure 6B) was approximately 30  $\text{mm}^3$ , compared to approximately 254  $\text{mm}^3$  in the severe TBI cohort (figure 2C, middle panel).

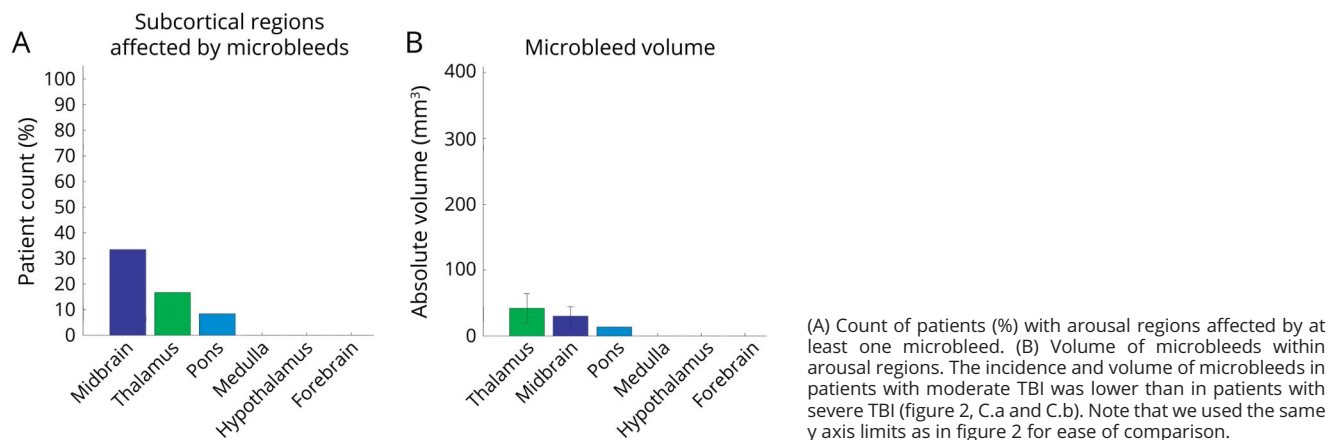
## Discussion

We identified multiple combinations of brainstem, thalamic, and hypothalamic microbleeds in patients with severe TBI who presented in coma and recovered consciousness within 6 months. There was no single arousal nucleus whose injury was required for the pathogenesis of traumatic coma. Rather, microbleeds were observed in variable combinations within brainstem arousal nuclei of the mesopontine tegmentum (PTg, mRt-p1Rt, DR, PAG, isRt) and ventral midbrain (SN1, SN2, VTA-PBP). The involvement of the mesopontine tegmentum is consistent with prior studies of coma-causing lesions, which identified a focal lesion hot spot in this brainstem region.<sup>36–38</sup> The involvement of the ventral midbrain raises the possibility that microbleeds in this region may also contribute to coma pathogenesis in patients with severe TBI, potentially due to disruption of dopaminergic pathways emanating from the ventral tegmental area.<sup>39</sup>

Our findings demonstrate the resilience of arousal mechanisms in patients with traumatic coma, because all patients recovered consciousness despite the presence of microbleeds in subcortical arousal nuclei. This resilience may be attributable to partial lesioning of the arousal nuclei, which suggests that none of the neurotransmitter systems that contribute to arousal were completely disrupted. Moreover, resilience could



**Figure 6** Incidence and Volume of Microbleeds in Patients With Moderate Traumatic Brain Injury (TBI)



be related to redundancy of arousal pathways connecting brainstem nuclei to the thalamus, hypothalamus, basal forebrain, and cortex,<sup>5</sup> and to dense interconnectivity between brainstem nuclei.<sup>2</sup>

Animal and limited human studies suggest that distinct components of the arousal network subservise different functional aspects of arousal. For instance, the LPB modulates autonomic arousal based on changes in carbon dioxide<sup>40</sup>; the LC modulates aspects of cognition including attention, decision-making, and memory<sup>41</sup>; the PAG is involved in modulating wakeful arousal<sup>25,42</sup> as well as emotional, motor, and autonomic state control.<sup>43</sup> Thus, considering all 17 brainstem nuclei as homogeneous components of the arousal network is an oversimplification. Future studies with larger cohorts and complementary imaging methods (e.g., diffusion MRI and resting-state functional MRI) are needed to identify the specific contributions of each network component to recovery of arousal, and hence consciousness.

An unexpected neuroanatomic observation in this study was the high frequency of traumatic microbleeds in the nigral-ventral tegmental area complex. The pathophysiologic relevance of these ventral midbrain microbleeds to traumatic coma requires further study, particularly in patients who do not have additional microbleeds in the mesopontine tegmentum. Regardless of whether ventral midbrain microbleeds can cause coma in isolation, or only in combination with other lesions in the mesopontine tegmentum, their apparent association with traumatic coma in this study is consistent with prior evidence that dopaminergic ventral midbrain neurons contribute to arousal.<sup>5,28-33</sup> Interestingly, the midbrain was the only region that displayed microbleeds in the entire cohort, consistent with its well-established biomechanical susceptibility to linear and rotational acceleration during head trauma.<sup>44</sup>

An important limitation of this study is that a traumatic microbleed is consistent with, but does not prove, injury to

underlying axons and neurons.<sup>2,10,45</sup> Emerging radiologic<sup>10,45</sup> and histopathologic<sup>2,10</sup> evidence suggests that microvascular injury, with a resulting microbleed, may occur in the absence of axonal injury. Furthermore, the full extent of neuronal or axonal injury caused by a microbleed cannot be precisely defined by SWI, particularly in the brainstem, where a single microbleed may injure local neuronal cell bodies as well as axons projecting from distant brainstem neurons. Detection of traumatic microbleeds by SWI may also be confounded by susceptibility artifacts at air-tissue interfaces such as the skull base, which may explain the unexpected observation that there were no basal forebrain microbleeds in the severe TBI cohort. Collectively, these limitations of SWI highlight the need for complementary imaging techniques, such as diffusion MRI, to quantify the burden of axonal injury in individual patients with TBI.<sup>45,46</sup>

The present study is further limited by its small sample size, young cohort age, and lack of patients with prolonged disorders of consciousness. Future work should account for the potential contribution of hemispheric microbleeds to coma pathogenesis, as we focused here on subcortical regions that contribute to arousal in the human brain.<sup>5-7</sup> It is also important to consider that unlike focal coma-causing brainstem lesions related to ischemic stroke or hypertensive hemorrhage,<sup>36,37</sup> traumatic microbleeds in the brainstem and diencephalon are never isolated. Rather, biomechanical, histopathologic, and neuroimaging studies<sup>22,44,47</sup> have demonstrated that traumatic microbleeds within the brainstem and diencephalon are invariably accompanied by axonal injury in the cerebral hemispheres. This diffuse, or multifocal, nature of axonal injury in patients with severe TBI precludes definitive conclusions about whether subcortical microbleeds cause coma.

We provide evidence for the resilience of arousal mechanisms in the human brain after severe TBI. We show that multiple combinations of subcortical microbleeds are associated with coma pathogenesis and are compatible with

recovery of consciousness. Our results also indicate that full recovery of consciousness by 6 months postinjury is common in patients with severe TBI who have brainstem microbleeds (i.e., grade 3 diffuse axonal injury). We recommend that SWI microbleed mapping be integrated with multimodal neuroimaging techniques in future studies to identify the specific components of the ascending arousal network that are necessary and sufficient for recovery of consciousness after traumatic coma.

## Acknowledgment

The authors thank Dr. Salvatore Nigro (Neuroscience Centre, Magna Graecia University, Catanzaro, Italy) for providing a mask of the pons in MNI space.

## Study Funding

This work was funded by grants from the NIH (NIBIB-K01EB019474, NIDCD-R21DC015888, NICHD-DP2HD 101400, NINDS-R21NS109627, NINDS-RF1NS115268, NIAR01AG063982), James S. McDonnell Foundation, Rappaport Foundation, and Tiny Blue Dot Foundation.

## Disclosure

The authors report no disclosures relevant to the manuscript. Go to [Neurology.org/N](http://Neurology.org/N) for full disclosures.

## Publication History

Received by *Neurology* December 3, 2020. Accepted in final form April 9, 2021.

## Appendix Authors

Name	Location	Contribution
<b>Marta Bianciardi, PhD</b>	Department of Radiology, Athinoula A. Martinos Center for Biomedical Imaging, Massachusetts General Hospital and Harvard Medical School, Boston	Conceived and designed the study, secured funding, preprocessed and analyzed the data, wrote the manuscript
<b>Saef Izzy, MD</b>	Department of Neurology, Brigham and Women's Hospital and Harvard Medical School, Boston, MA	Preprocessed and analyzed the data, wrote the manuscript
<b>Bruce R. Rosen, MD, PhD</b>	Department of Radiology, Athinoula A. Martinos Center for Biomedical Imaging, Massachusetts General Hospital and Harvard Medical School, Boston	Conceived and designed the study, provided feedback throughout the process
<b>Lawrence L. Wald, PhD</b>	Department of Radiology, Athinoula A. Martinos Center for Biomedical Imaging, Massachusetts General Hospital and Harvard Medical School, Boston	Conceived and designed the study, provided feedback throughout the process
<b>Brian L. Edlow, MD</b>	Center for Neurotechnology and Neurorecovery, Department of Neurology, Massachusetts General Hospital and Harvard Medical School, Boston	Conceived and designed the study, secured funding, performed data acquisition, preprocessed and analyzed the data, wrote the manuscript

## References

- Rosenblum WI. Immediate, irreversible, posttraumatic coma: a review indicating that bilateral brainstem injury rather than widespread hemispheric damage is essential for its production. *J Neuropathol Exp Neurol.* 2015;74(3):198-202.
- Edlow BL, Haynes RL, Takahashi E, et al. Disconnection of the ascending arousal system in traumatic coma. *J Neuropathol Exp Neurol.* 2013;72(6):505-523.
- Snider SB, Bodien YG, Bianciardi M, Brown EN, Edlow BL. Disruption of the ascending arousal network in acute traumatic disorders of consciousness. *Neurology.* 2019;93(13):e1281-e1287.
- Snider SB, Bodien YG, Frau-Pascual A, Bianciardi M, Foulkes AS, Edlow BL. Ascending arousal network connectivity during recovery from traumatic coma. *Neuroimage Clin.* 2020;28:102503.
- Parvizi J, Damasio A. Consciousness and the brainstem. *Cognition.* 2001;79(1-2):135-160.
- Saper CB, Chou TC, Scammell TE. The sleep switch: hypothalamic control of sleep and wakefulness. *Trends Neurosci.* 2001;24(12):726-731.
- Brown EN, Lydic R, Schiff ND. General anesthesia, sleep, and coma. *N Engl J Med.* 2010;363:2638-2650.
- Izzy S, Compton R, Carandang R, et al. Self-fulfilling prophecies through withdrawal of care: do they exist in traumatic brain injury, too? *Neurocrit Care.* 2013;19:347-363.
- Turgeon AF, Lauzier F, Simard JF, et al; Canadian Critical Care Trials Group. Mortality associated with withdrawal of life-sustaining therapy for patients with severe traumatic brain injury: a Canadian multicentre cohort study. *CMAJ.* 2011;183:1581-1588.
- Griffin AD, Turtzo LC, Parikh GY, et al. Traumatic microbleeds suggest vascular injury and predict disability in traumatic brain injury. *Brain.* 2019;142:3550-3564.
- Edlow BL, Claassen J, Schiff ND, Greer DM. Recovery from disorders of consciousness: mechanisms, prognosis and emerging therapies. *Nat Rev Neurol.* 2021;17:135-156.
- Jennett B. Defining brain damage after head injury. *J R Coll Physicians Lond.* 1979;13(4):197-200.
- Maas AI, Roozenbeek B, Manley GT. Clinical trials in traumatic brain injury: past experience and current developments. *Neurotherapeutics.* 2010;7(1):115-126.
- Sokolik R, Degano G, Banellis L, et al. Covert speech comprehension predicts recovery from acute unresponsive states. *Ann Neurol.* 2020;89(4):646-656.
- Lawrence TP, Pretorius PM, Ezra M, Cadoux-Hudson T, Voets NL. Early detection of cerebral microbleeds following traumatic brain injury using MRI in the hyper-acute phase. *Neurosci Lett.* 2017;655:143-150.
- Greenberg SM, Vernooij MW, Cordonnier C, et al; Microbleed Study Group. Cerebral microbleeds: a guide to detection and interpretation. *Lancet Neurol.* 2009;8:165-174.
- Desikan RS, Ségonne F, Fischl B, et al. An automated labeling system for subdividing the human cerebral cortex on MRI scans into gyral based regions of interest. *Neuroimage.* 2006;31:968-980.
- Pauli WM, Nili AN, Tyszka JM. A high-resolution probabilistic in vivo atlas of human subcortical brain nuclei. *Sci Data.* 2018;5:180063.
- Nigro S, Cerasa A, Zito G, et al. Fully automated segmentation of the pons and midbrain using human T1 MR brain images. *PLoS One.* 2014;9:e85618.
- Destrieux C, Fischl B, Dale A, Halgren E. Automatic parcellation of human cortical gyri and sulci using standard anatomical nomenclature. *Neuroimage.* 2010;53:1-15.
- Bianciardi M, Strong C, Toschi N, et al. A probabilistic template of human mesopontine tegmental nuclei from in vivo 7T MRI. *Neuroimage.* 2018;170:222-230.
- Izzy S, Mazwi NL, Martinez S, et al. Revisiting grade 3 diffuse axonal injury: not all brainstem microbleeds are prognostically equal. *Neurocrit Care.* 2017;27:199-207.
- Mazwi NL, Izzy S, Tan CO, et al. Traumatic microbleeds in the hippocampus and corpus callosum predict duration of posttraumatic amnesia. *J Head Trauma Rehabil.* 2019;34:E10-E18.
- Moruzzi G, Magoun HW. Brain stem reticular formation and activation of the EEG. *Electroencephalogr Clin Neurophysiol.* 1949;1:455-473.
- Saper CB, Fuller PM, Pedersen NP, Lu J, Scammell TE. Sleep state switching. *Neuron.* 2010;68:1023-1042.
- Fuller PM, Fuller P, Sherman D, Pedersen NP, Saper CB, Lu J. Reassessment of the structural basis of the ascending arousal system. *J Comp Neurol.* 2011;519:933-956.
- Munk MH, Roelfsema PR, König P, Engel AK, Singer W. Role of reticular activation in the modulation of intracortical synchronization. *Science.* 1996;272:271-274.
- Eban-Rothschild A, Rothschild G, Giardino WJ, Jones JR, de Lecea L. VTA dopaminergic neurons regulate ethologically relevant sleep-wake behaviors. *Nat Neurosci.* 2016;19:1356-1366.
- Monti JM, Jantos H. The roles of dopamine and serotonin, and of their receptors, in regulating sleep and waking. *Prog Brain Res.* 2008;172:625-646.
- Lima MM, Andersen ML, Reksidler AB, Vital MA, Tufik S. The role of the substantia nigra pars compacta in regulating sleep patterns in rats. *PLoS One.* 2007;2:e513.
- Lima MMS, Reksidler AB, Vital MABF. The dopaminergic dilemma: sleep or wake? Implications in Parkinson's disease. *Biosci Hypothesis.* 2008;1:9-13.
- Datta S, Curró Dossi R, Paré D, Oakson G, Steriade M. Substantia nigra reticulata neurons during sleep-waking states: relation with ponto-geniculo-occipital waves. *Brain Res.* 1991;566:344-347.
- Olszewski J, Baxter D. *Cytoarchitecture of the Human Brainstem.* JB Lippincott; 2014.
- Bianciardi M, Toschi N, Edlow BL, et al. Toward an in vivo neuroimaging template of human brainstem nuclei of the ascending arousal, autonomic, and motor systems. *Brain Connect.* 2015;5:597-607.
- Singh K, Indovina I, Augustinack J, et al. Probabilistic template of the lateral parabrachial nucleus, medial parabrachial nucleus, vestibular nuclei complex, and

- medullary viscerosensory-motor nuclei complex in living humans from 7 Tesla MRI. *Front Neurosci.* 2020;13:1425.
36. Fischer DB, Boes AD, Demertzi A, et al. A human brain network derived from coma-causing brainstem lesions. *Neurology.* 2016;87:2427-2434.
  37. Parvizi J, Damasio AR. Neuroanatomical correlates of brainstem coma. *Brain.* 2003;126:1524-1536.
  38. Snider SB, Hsu J, Darby RR, et al. Cortical lesions causing loss of consciousness are anticorrelated with the dorsal brainstem. *Hum Brain Mapp.* 2020;41:1520-1531.
  39. Edlow BL, Barra ME, Zhou DW, et al. Personalized connectome mapping to guide targeted therapy and promote recovery of consciousness in the intensive care unit. *Neurocrit Care.* 2020;33:364-375.
  40. Kaur S, Pedersen NP, Yokota S, et al. Glutamatergic signaling from the parabrachial nucleus plays a critical role in hypercapnic arousal. *J Neurosci.* 2013;33(18):7627-7640.
  41. Sara SJ. The locus coeruleus and noradrenergic modulation of cognition. *Nat Rev Neurosci.* 2009;10(3):211-223.
  42. Lu J, Jhou TC, Saper CB. Identification of wake-active dopaminergic neurons in the ventral periaqueductal gray matter. *J Neurosci.* 2006;26(1):193-202.
  43. Carrive P, Morgan MM. Periaqueductal gray. In: Paxinos G, Mai JK, eds. *The Human Nervous System*, ed. 3. Elsevier Academic Press; 2012.
  44. Ommaya AK, Gennarelli TA. Cerebral concussion and traumatic unconsciousness: correlation of experimental and clinical observations of blunt head injuries. *Brain.* 1974;97:633-654.
  45. Jolly AE, Bălăeș M, Azor A, et al. Detecting axonal injury in individual patients after traumatic brain injury. *Brain.* 2021;144:92-113.
  46. Nolan AL, Petersen C, Iacono D, et al. Tractography-pathology correlations in traumatic brain injury: a TRACK-TBI study. *J Neurotrauma.* 2021. doi: 10.1089/neu.2020.7373
  47. Adams JH, Doyle D, Ford I, Gennarelli TA, Graham DI, McLellan DR. Diffuse axonal injury in head injury: definition, diagnosis and grading. *Histopathology.* 1989;15:49-59.